ICP-MS
INDUCTIVELY COUPLED PLASMA
MASS SPECTROMETRY
(SPETTROMETRIA DI MASSA A PLASMA ACCOPPIATO INDUTTIVAMENTE)

Mass Spectrometry

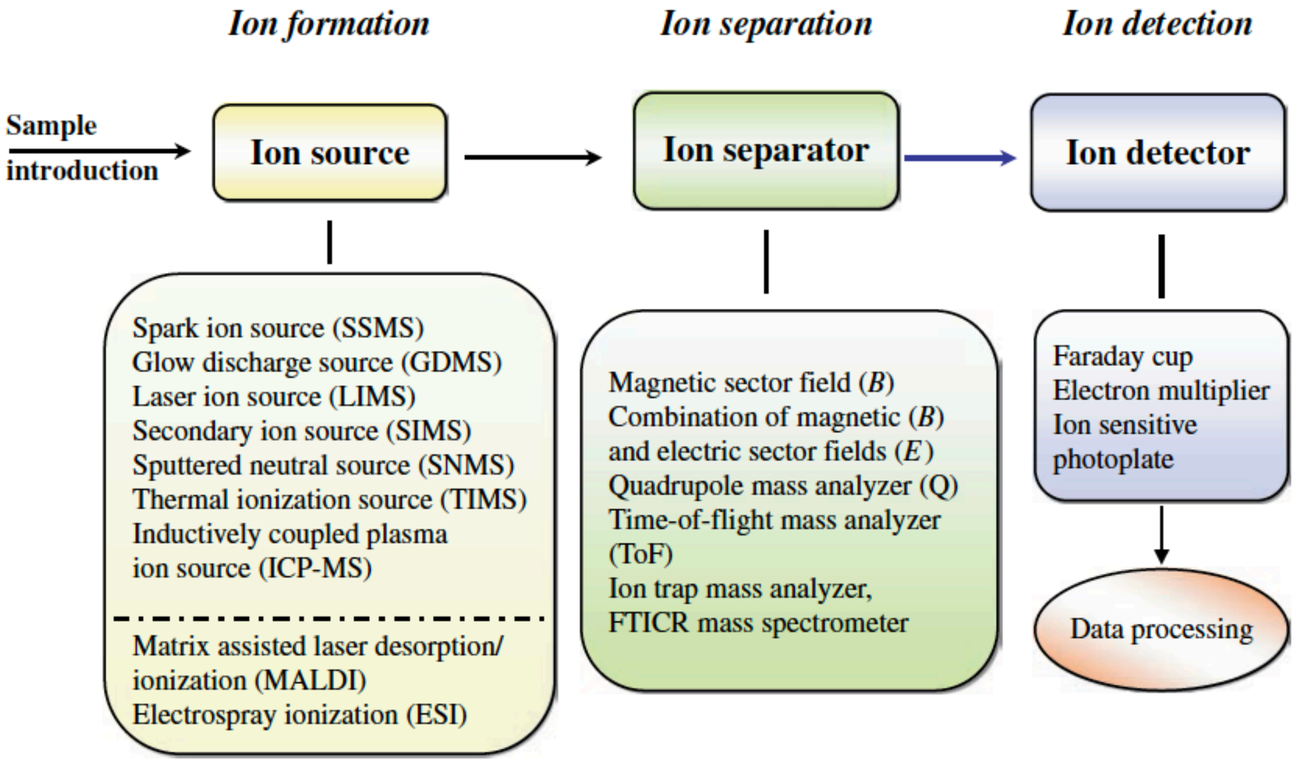

Figure 1.1 *Basic diagram of mass spectrometry: generation of ions from compounds in the sample, introduction into the ion source, separation of these ions by their mass-to-charge ratio in the mass separator and detection of ions in the ion detector.*

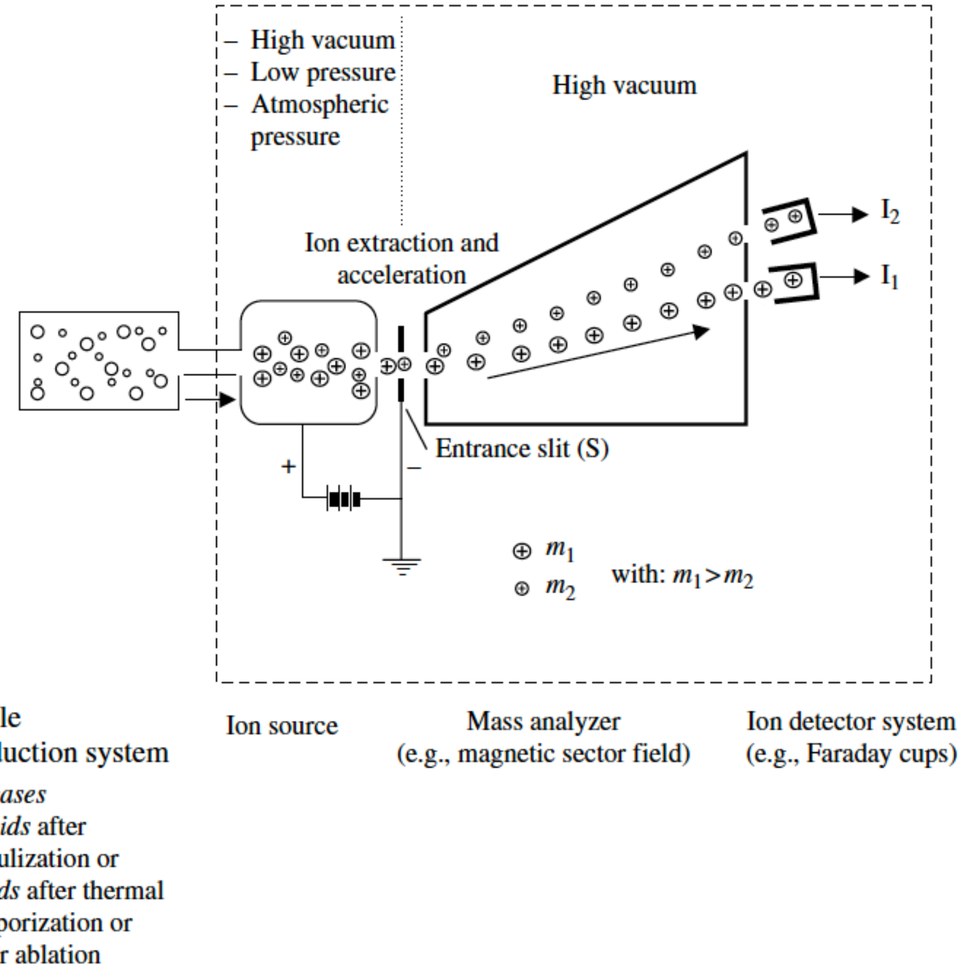

Figure 1.2 *Principle of the operation of a mass spectrometer including sample introduction system, ion source, mass separator (e.g., a magnetic sector field) and ion detector system (e.g., double ion collectors for simultaneous measurements of two separated ion beams).*

Mass Spectrometry

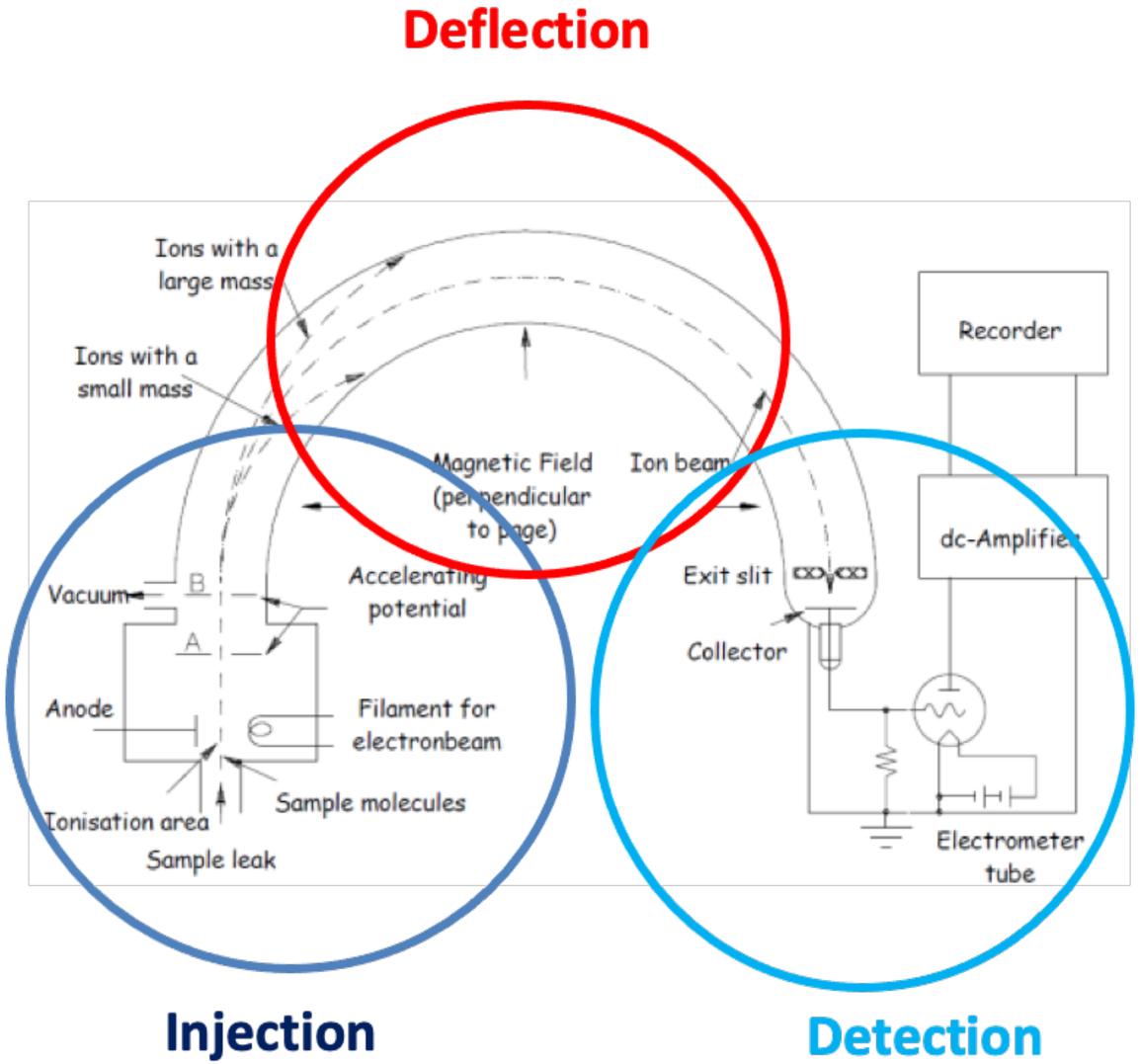

Sorgente di ioni

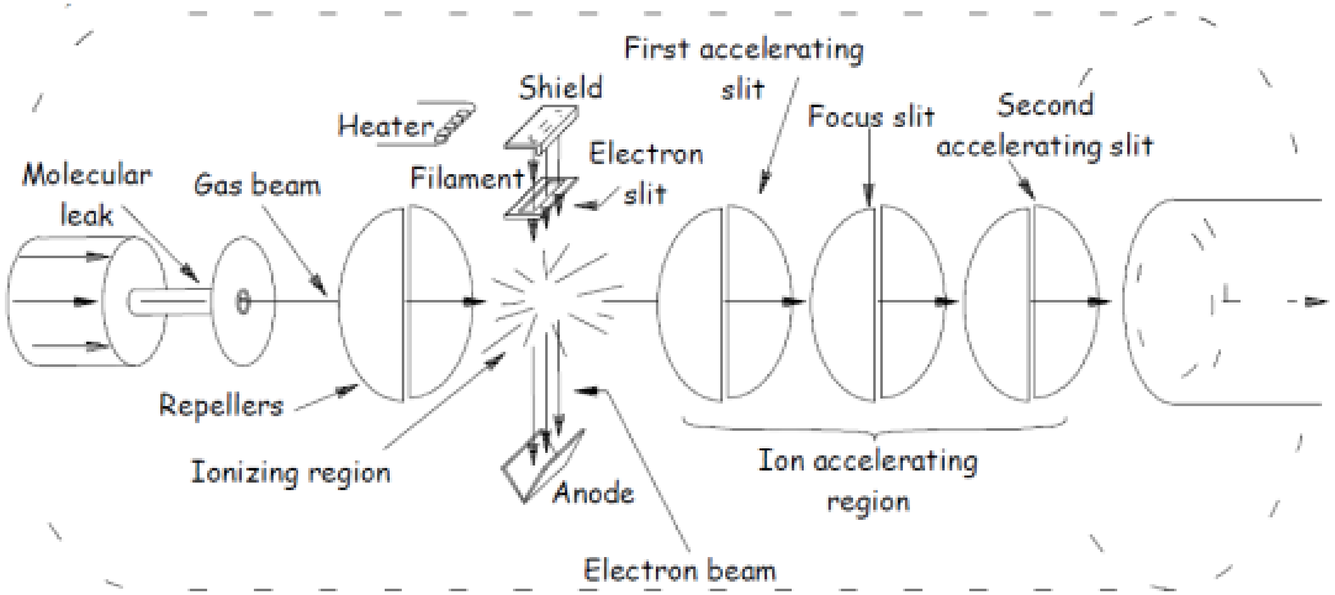

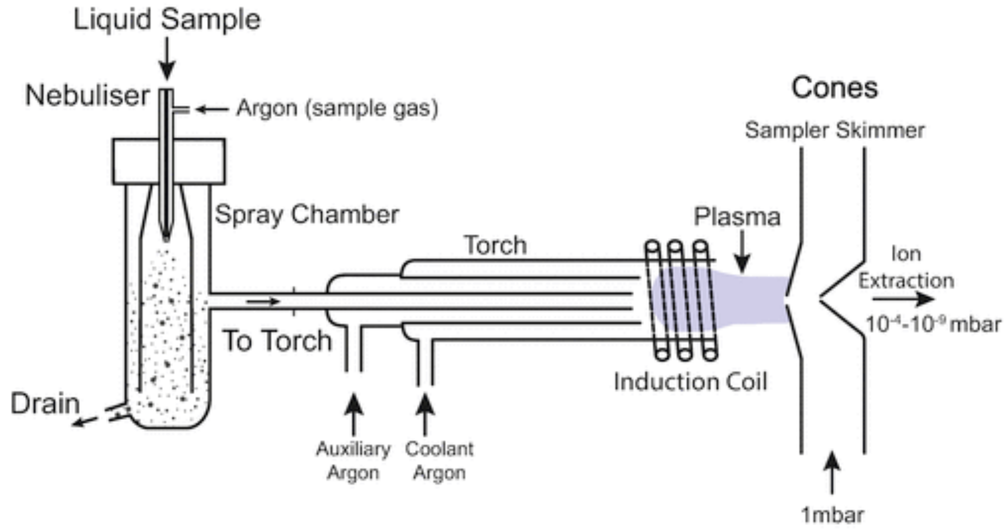

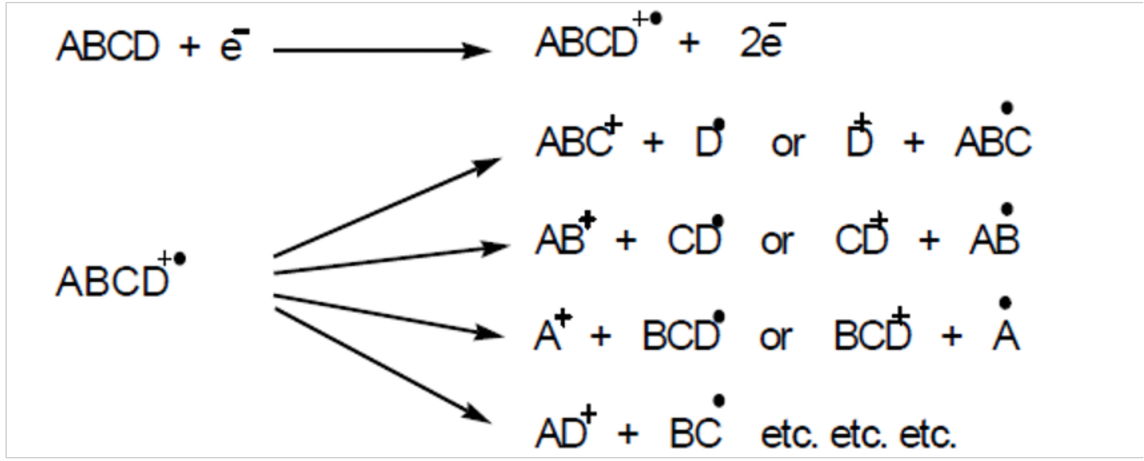

Introduzione del campione

Nebulizzazione

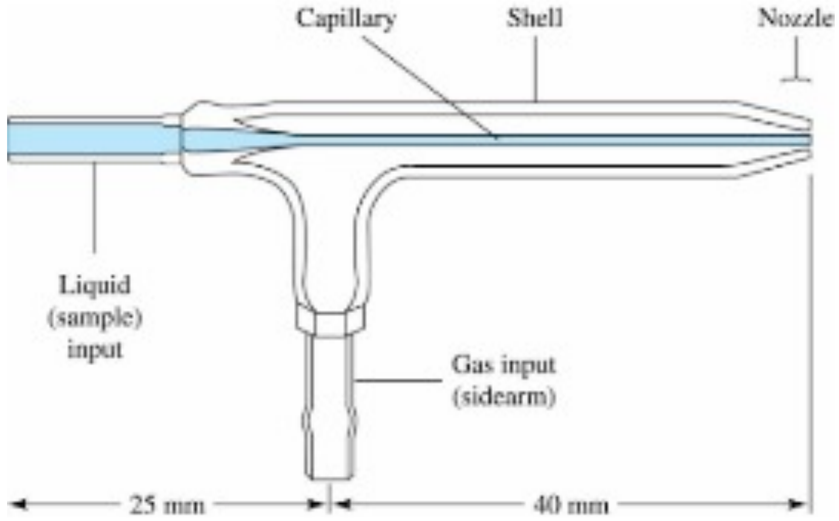

Ablazione laser

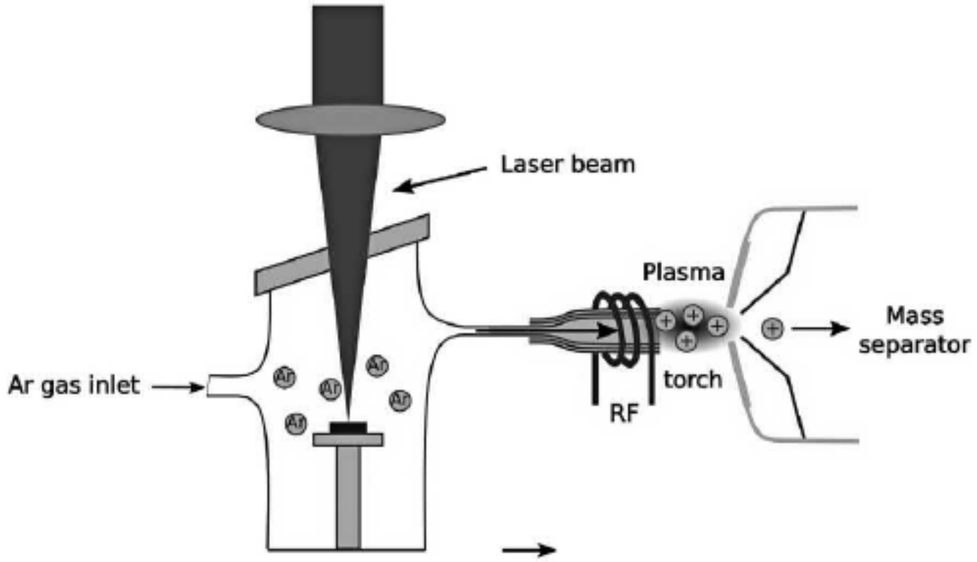

Laser ablation ICP-MS

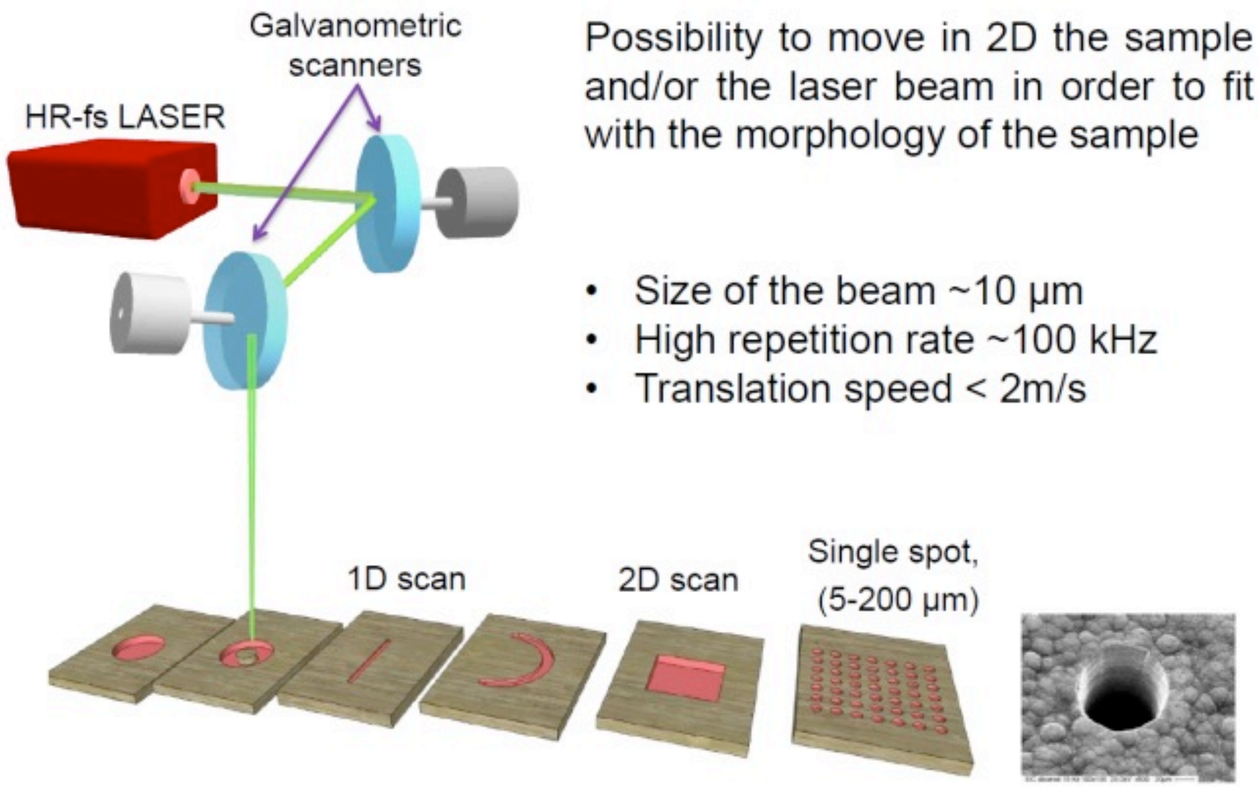

Possibility to move in 2D the sample and/or the laser beam in order to fit with the morphology of the sample

- Size of the beam ~10 µm
- High repetition rate ~100 kHz
- Translation speed < 2m/s

Laser ablation ICP-MS

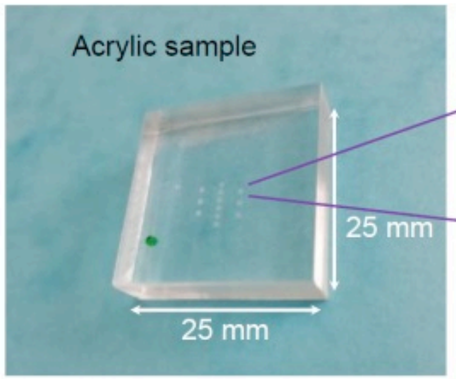

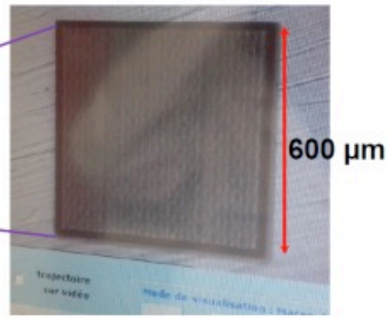

2D scan of a square of 600x600 µm^2
with a laser spot of 8 µm

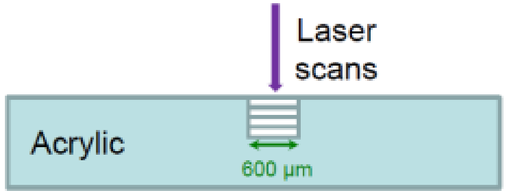

Several 2D laser scans
to explore the Z-axis

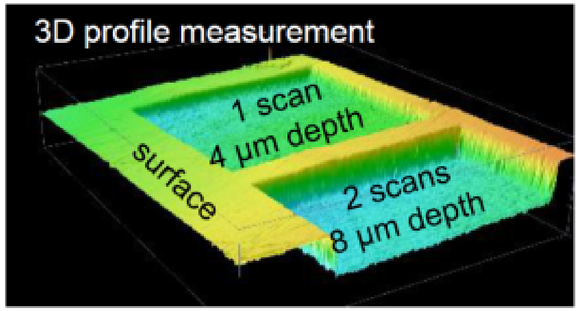

Settore magnetico e settore elettrostatico

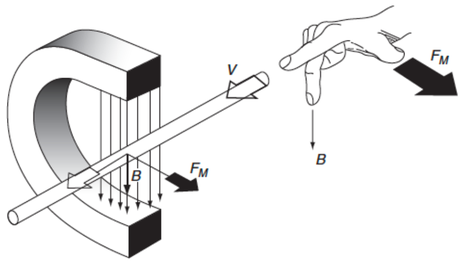

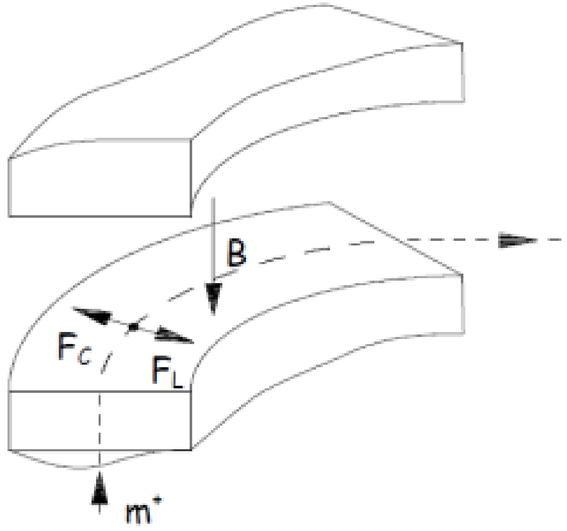

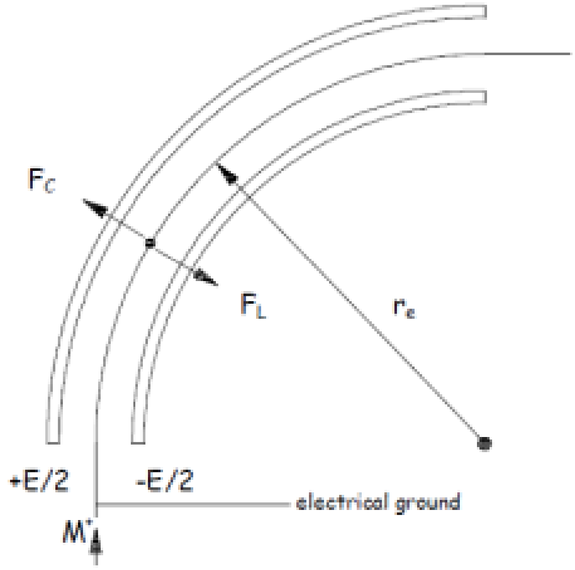

Settore magnetico e settore elettrostatico

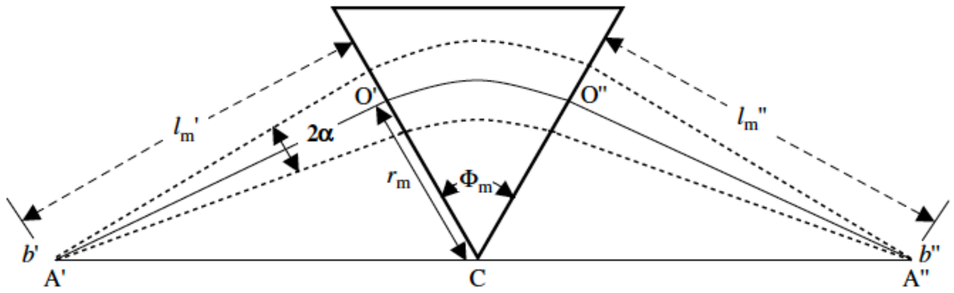

Figure 3.1 *Focusing properties (lens effect) of a homogeneous magnetic field for mass separation of ion beams. A′, A″ and C are the positions of the object, image and centre of curvature, respectively, l_m' and l_m'' are the distances of object and image, respectively, from the boundaries of the magnetic field. Φ_m is the angle of the sector field. The ions which were injected from object A′ having a half-angular direction spread α are focused at the image point A″. Parameters b′ and b″ are used to describe the real object and image widths of the entrance and exit slits (A′ and A″), respectively.*

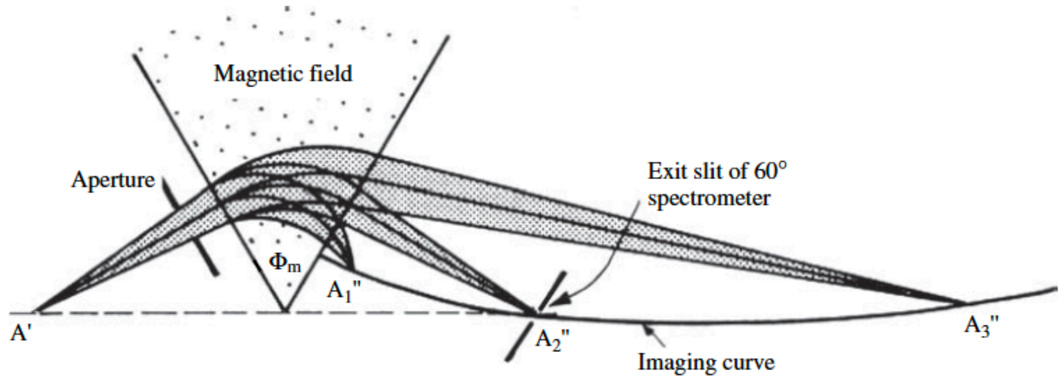

Figure 3.3 *Prism effect of a homogeneous sector field with angle Φ_m. Ions flying perpendicularly from the entrance point A′ in a magnetic sector field, separating in this magnetic sector field into three ion beams A_1'', A_2'' and A_3'', (with different m/z ratios), focusing on the imaging curve. The exit slit of the magnetic field is installed on the imaging curve at point A_2''. (H. Kienitz (ed.), Massenspektrometrie (1968), Verlag Chemie, Weinheim. Reproduced by permission of Wiley-VCH)*

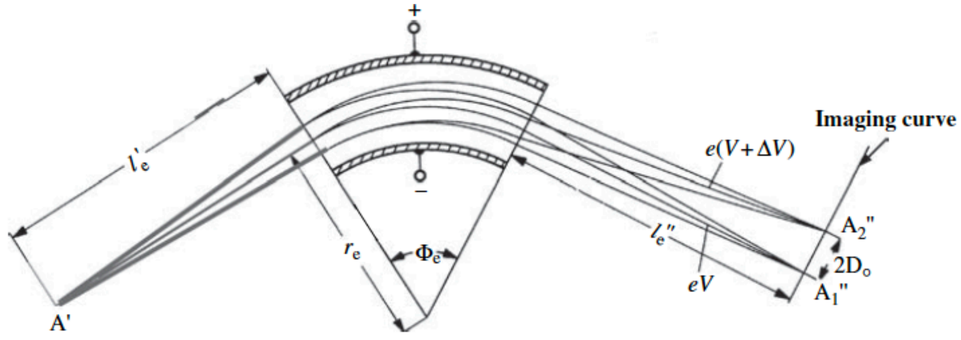

Figure 3.4 *Prism and lens effect of an electric sector field with radius r_e and sector angle Φ_e. The ions coming from the ion-emitting point A′ enter the electric sector field after a distance of l_e' and are focused on the imaging curve behind the electric sector field at a distance of l_e''. Ions of energy $e(V+\Delta V)$ and $e(V-\Delta V)$ are focused in two separate images A_1'' and A_2''. (Massenspektrometrie Herausgegeben, Von Kienitz, H., Verlag Chemie, GmbH, Weinheim (1968). Reproduced by permission of Wiley-VCH)*

Doppia focalizzazione (double focusing)

Figure 2.53
Combination of the two sectors, electrical and magnetic, shown in Figure 2.52; the magnetic sector is turned over so as to obtain double focusing.

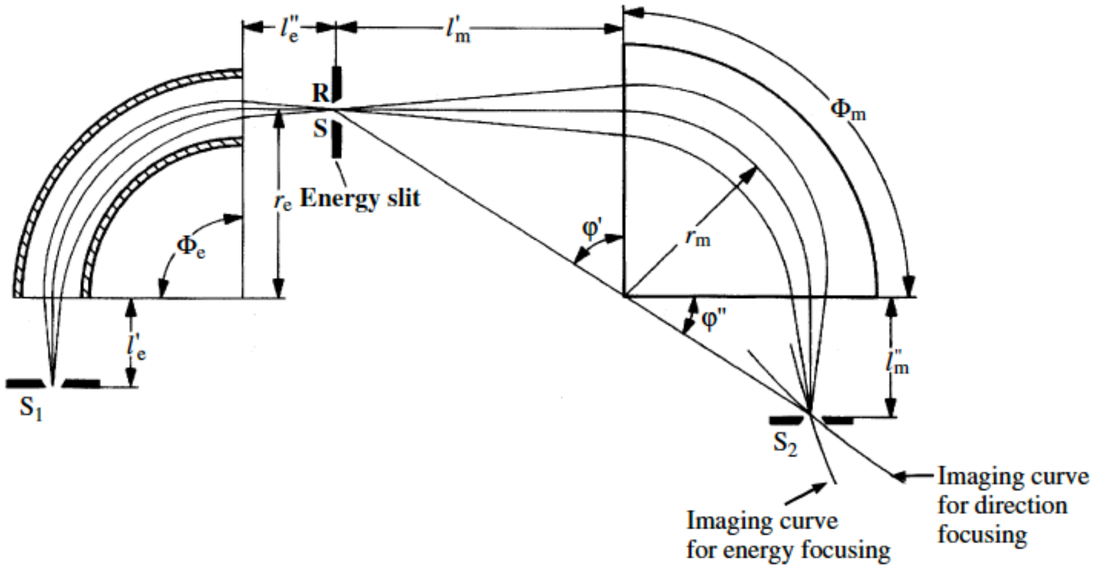

Figure 3.5 *Double-focusing sector field mass spectrometer with Nier–Johnson geometry. (H. Kienitz (ed.), Massenspektrometrie (1968), Verlag Chemie, Weinheim. Reproduced by permission of Wiley-VCH)*

Doppia focalizzazione (double focusing)

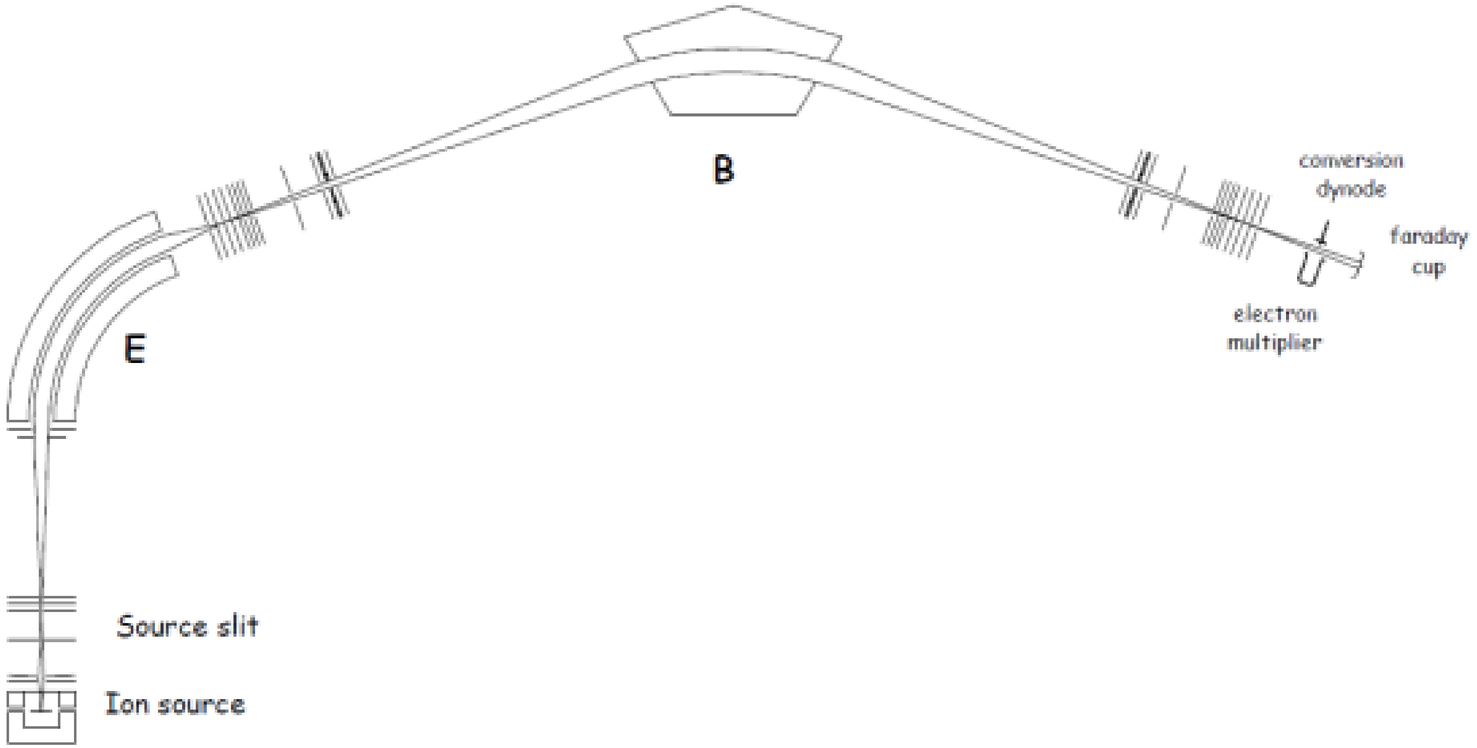

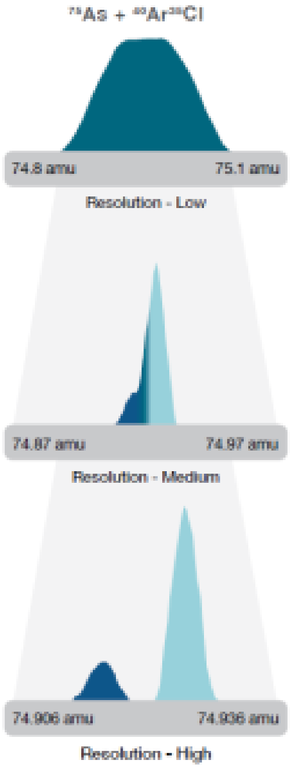

ICP-MS ad alta risoluzione

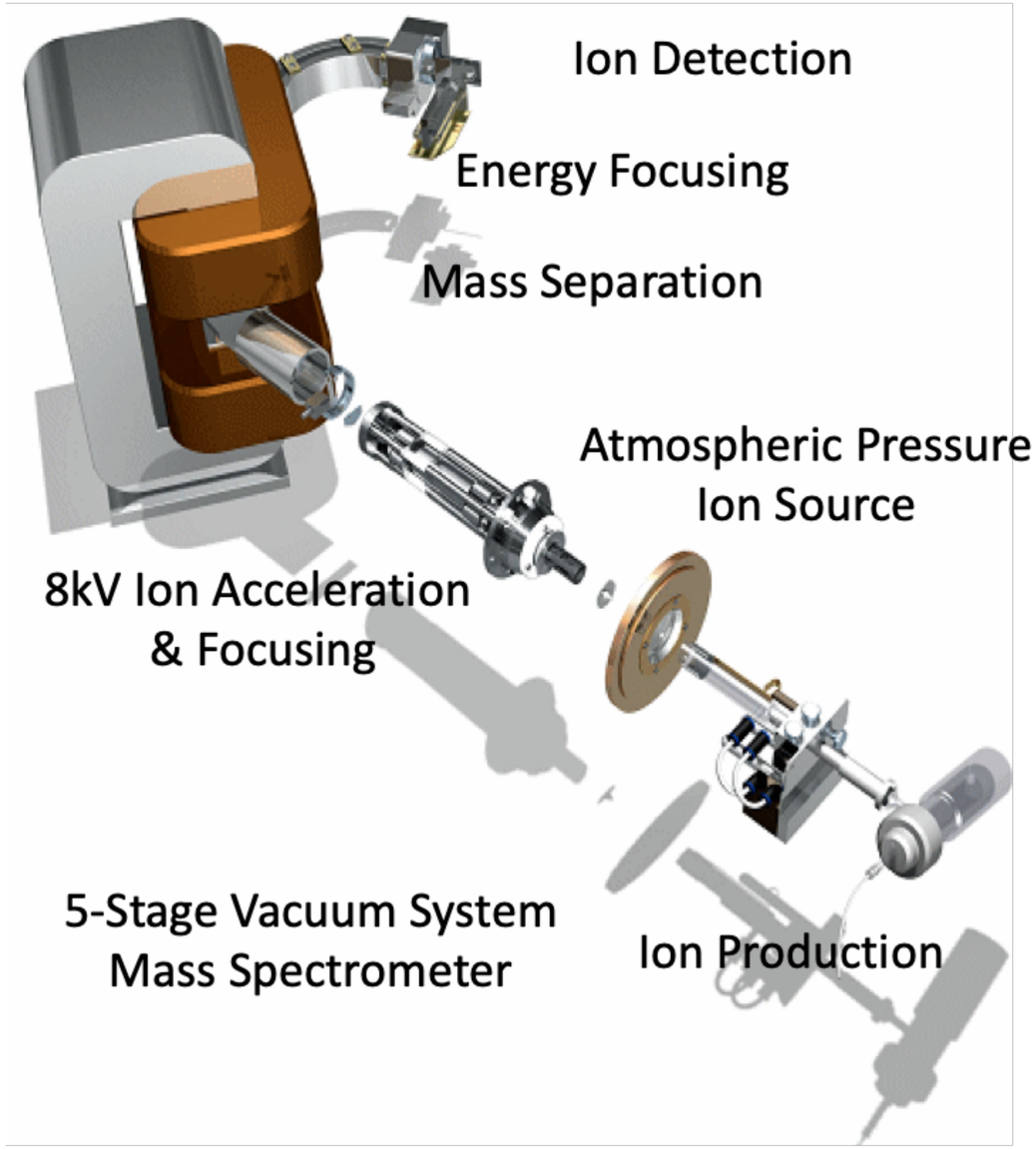

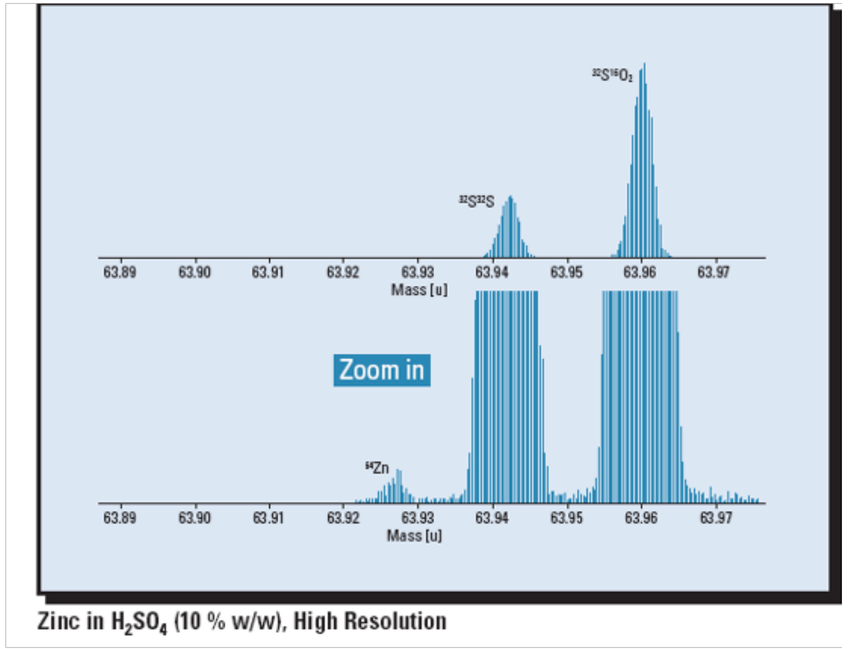

Zinc in H_2SO_4 (10 % w/w), High Resolution

ICP-MS ad alta risoluzione –> 40K

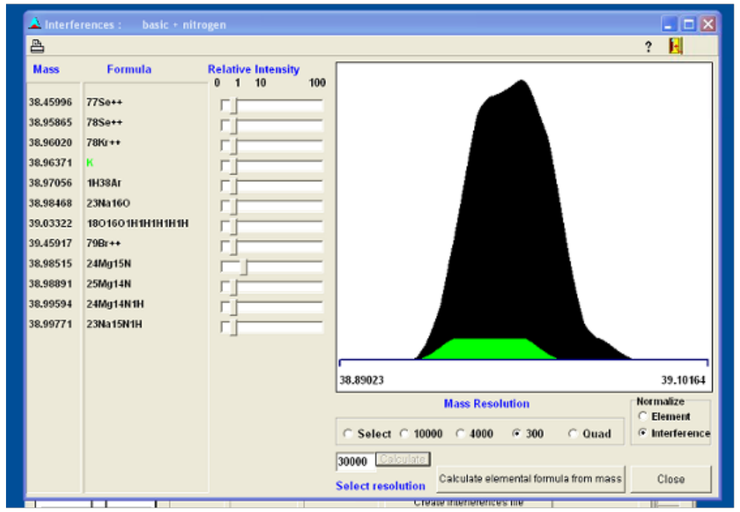

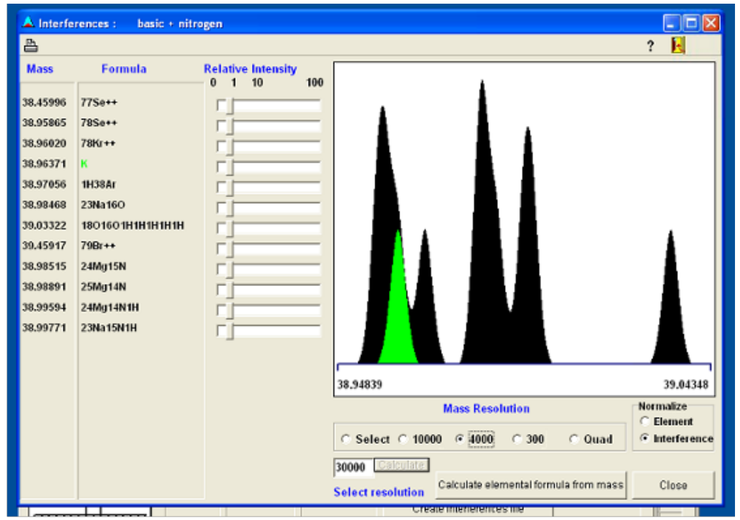

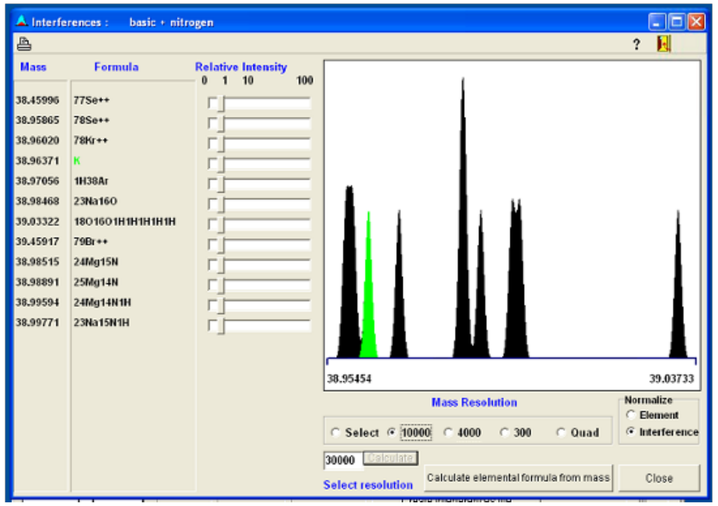

Multicollettore

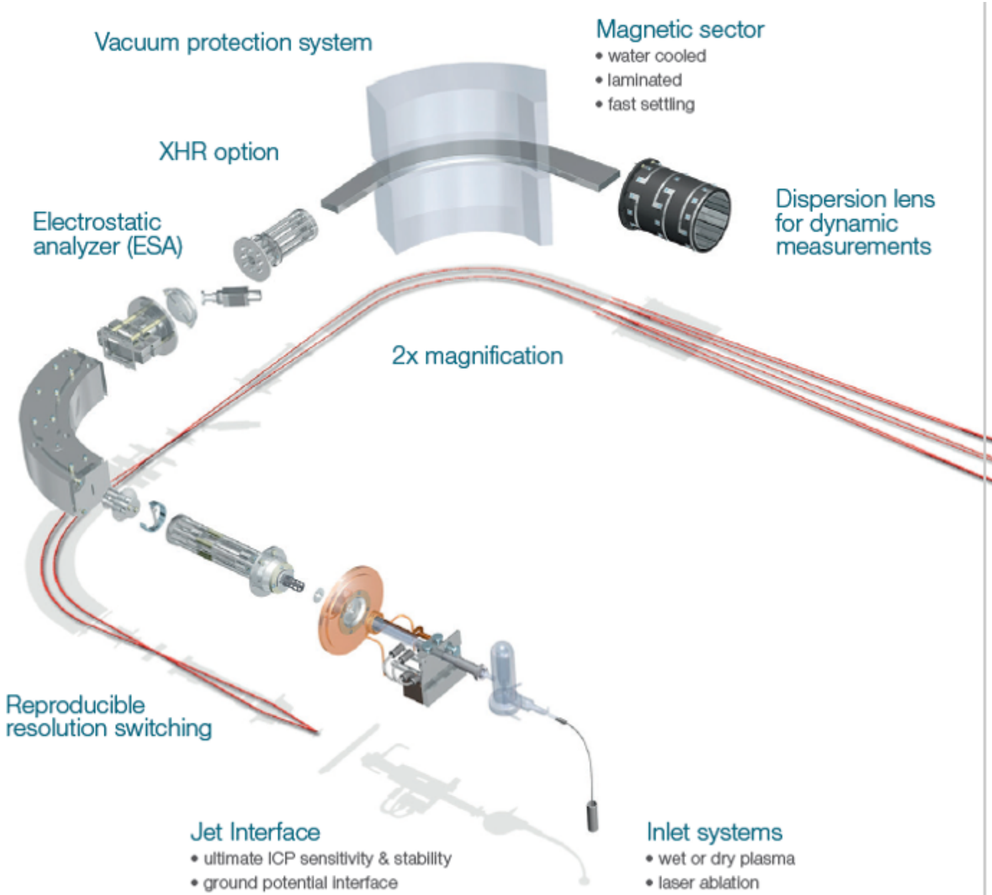

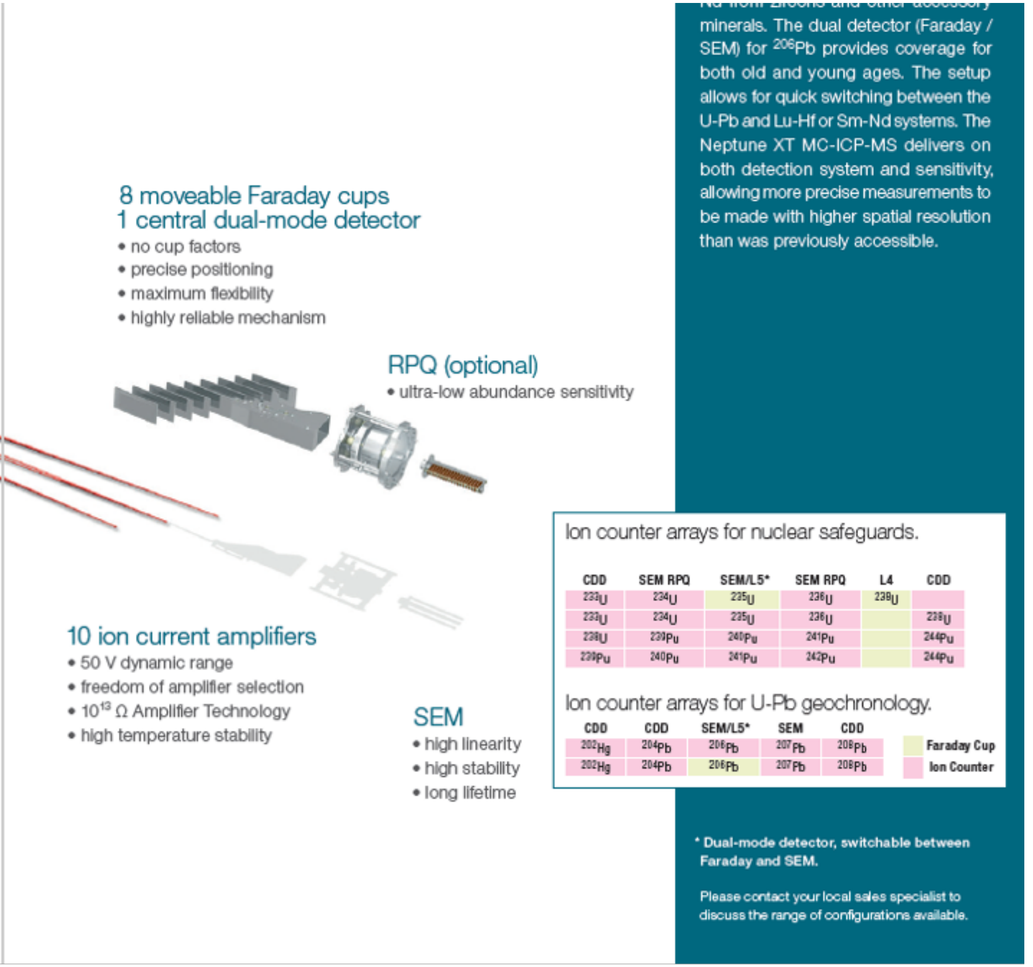

minerals. The dual detector (Faraday / SEM) for ^{206}Pb provides coverage for both old and young ages. The setup allows for quick switching between the U-Pb and Lu-Hf or Sm-Nd systems. The Neptune XT MC-ICP-MS delivers on both detection system and sensitivity, allowing more precise measurements to be made with higher spatial resolution than was previously accessible.

Ion counter arrays for nuclear safeguards.

CDD	SEM RPQ	SEM/L5*	SEM RPQ	L4	CDD
^{233}U	^{234}U	^{235}U	^{236}U	^{238}U	
^{233}U	^{234}U	^{235}U	^{236}U		^{238}U
^{238}U	^{239}Pu	^{240}Pu	^{241}Pu		^{244}Pu
^{239}Pu	^{240}Pu	^{241}Pu	^{242}Pu		^{244}Pu

Ion counter arrays for U-Pb geochronology.

CDD	CDD	SEM/L5*	SEM	CDD
^{202}Hg	^{204}Pb	^{206}Pb	^{207}Pb	^{208}Pb
^{202}Hg	^{204}Pb	^{206}Pb	^{207}Pb	^{208}Pb

Faraday Cup
Ion Counter

* Dual-mode detector, switchable between Faraday and SEM.

Please contact your local sales specialist to discuss the range of configurations available.

ICP-MS a quadrupolo

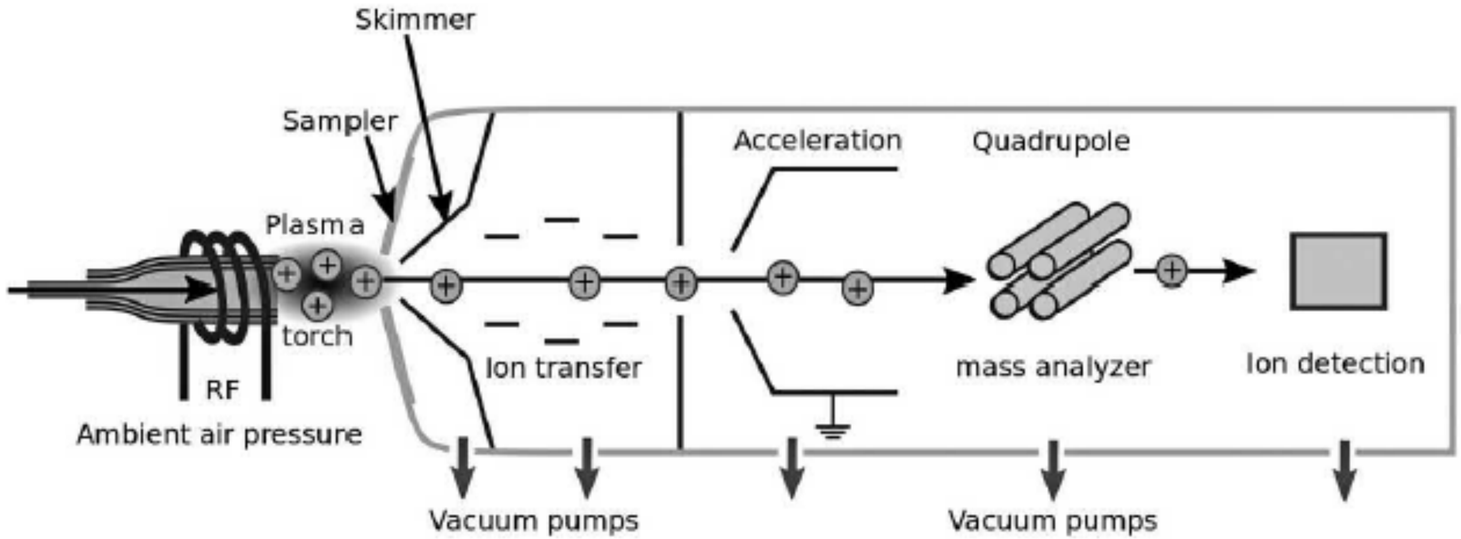

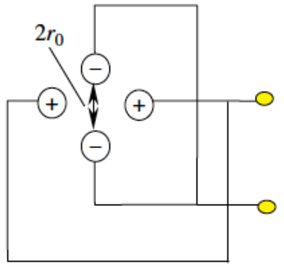

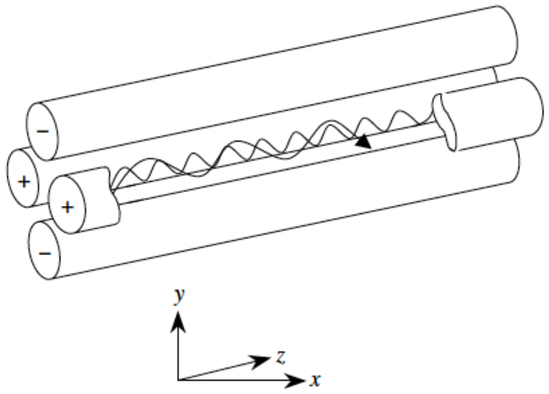

$U + V \cos \omega t$

U – dc voltage

$V \cos \omega t$ – rf voltage

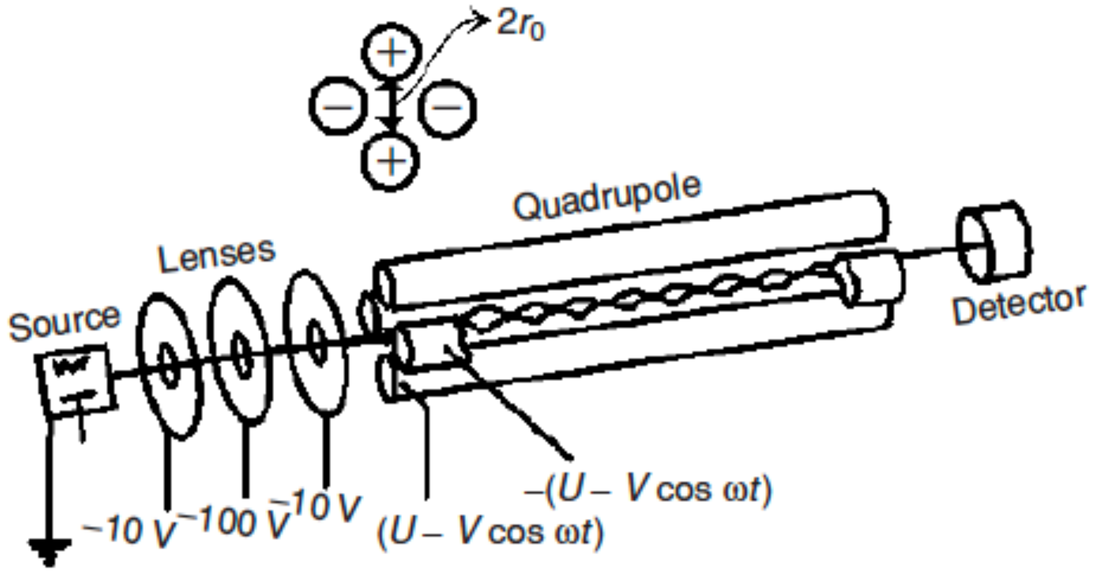

Figure 3.7 *Schematic and cross section of a linear quadrupole mass analyzer with cylindrical rod electrodes. (H. Kienitz (ed.), Massenspektrometrie (1968), Verlag Chemie, Weinheim. Reproduced by permission of Wiley-VCH)*

Preparazione dei campioni
Cromatografia

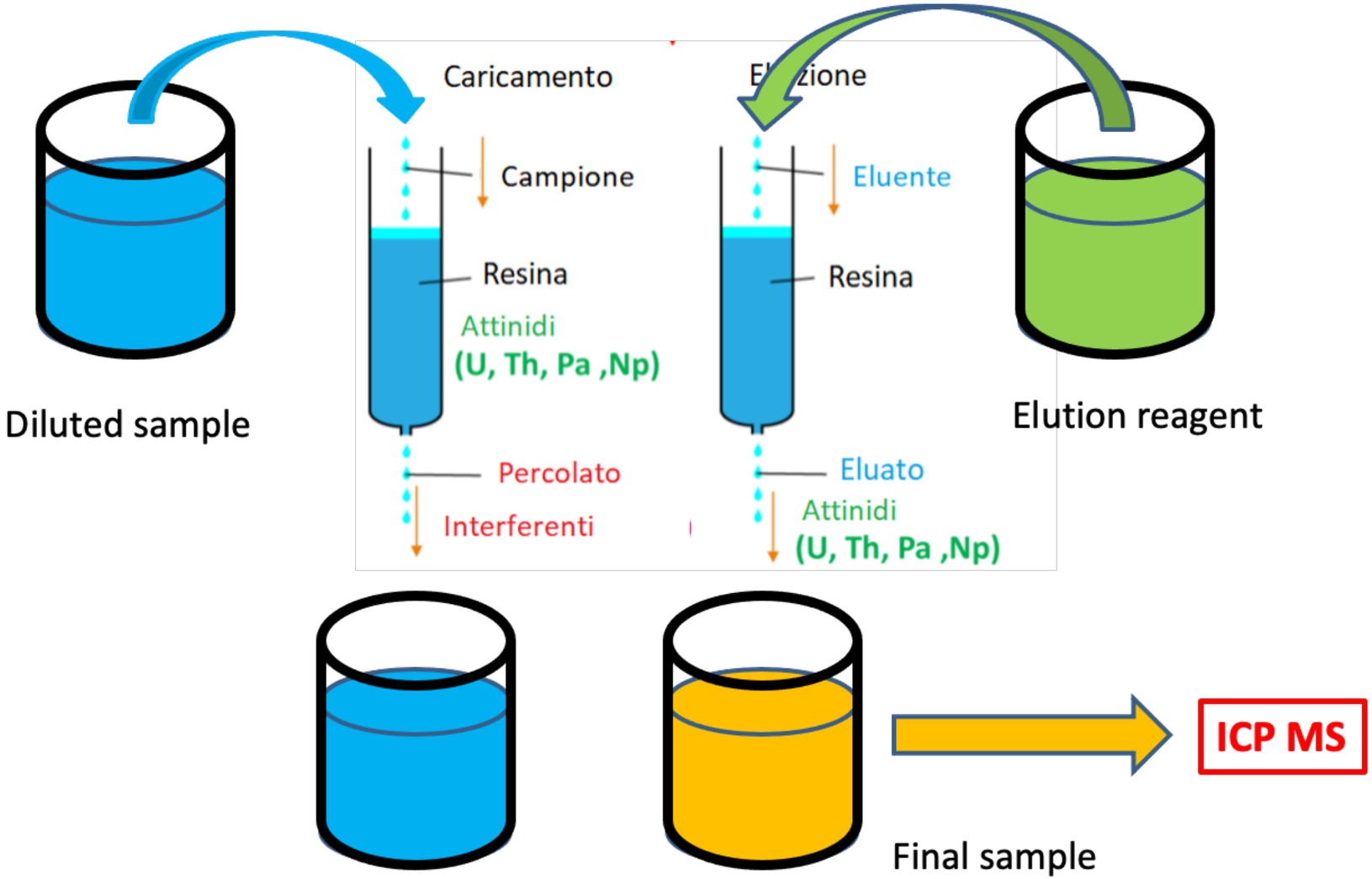

Resine cromatografiche

Retention

Elution

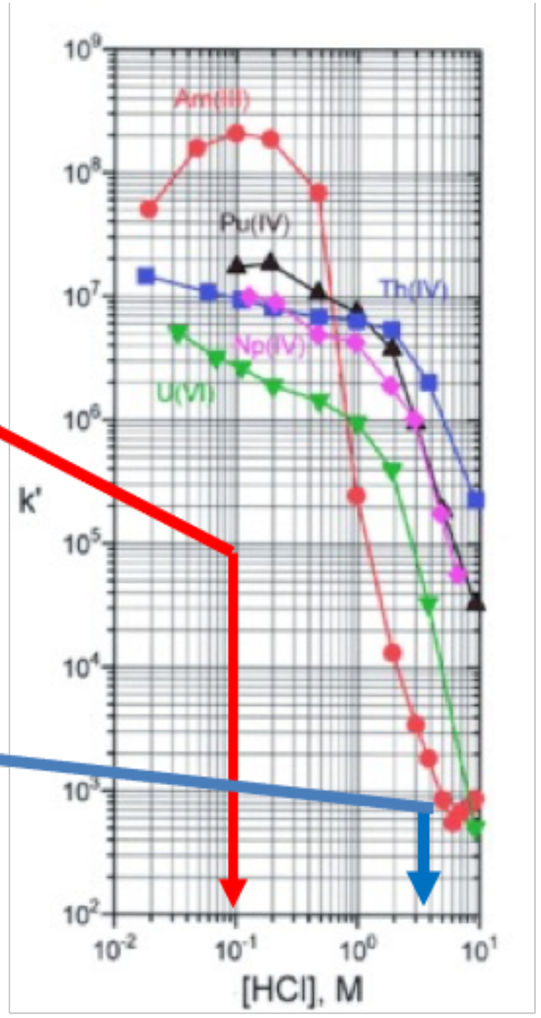

Resine per attinidi – HNO3

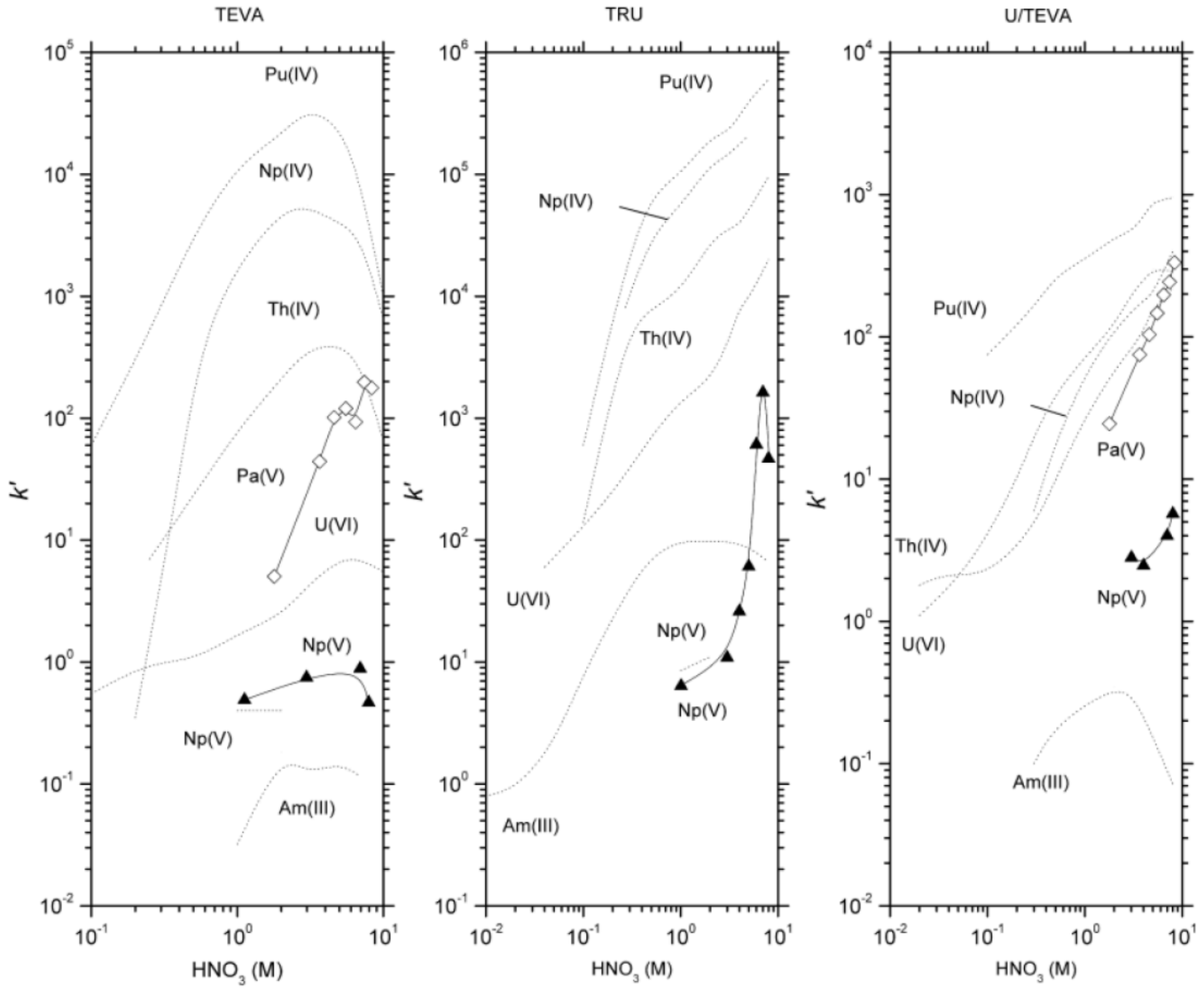

Fig. 3. HNO_3 dependencies of k' values for selected actinides with the TEVA, TRU and U/TEVA resins (T = 22–26° C; 100–150 μm particle size resins). Data for Np(V) k' values determined in this work are represented in filled triangles whereas values reported in dotted lines are extracted from Refs. [18,20]. U(VI), Np(IV), Th(IV), Pu(IV) and Am(III) k' values are extracted from Refs. [18–20].

Resine per attinidi – HCl

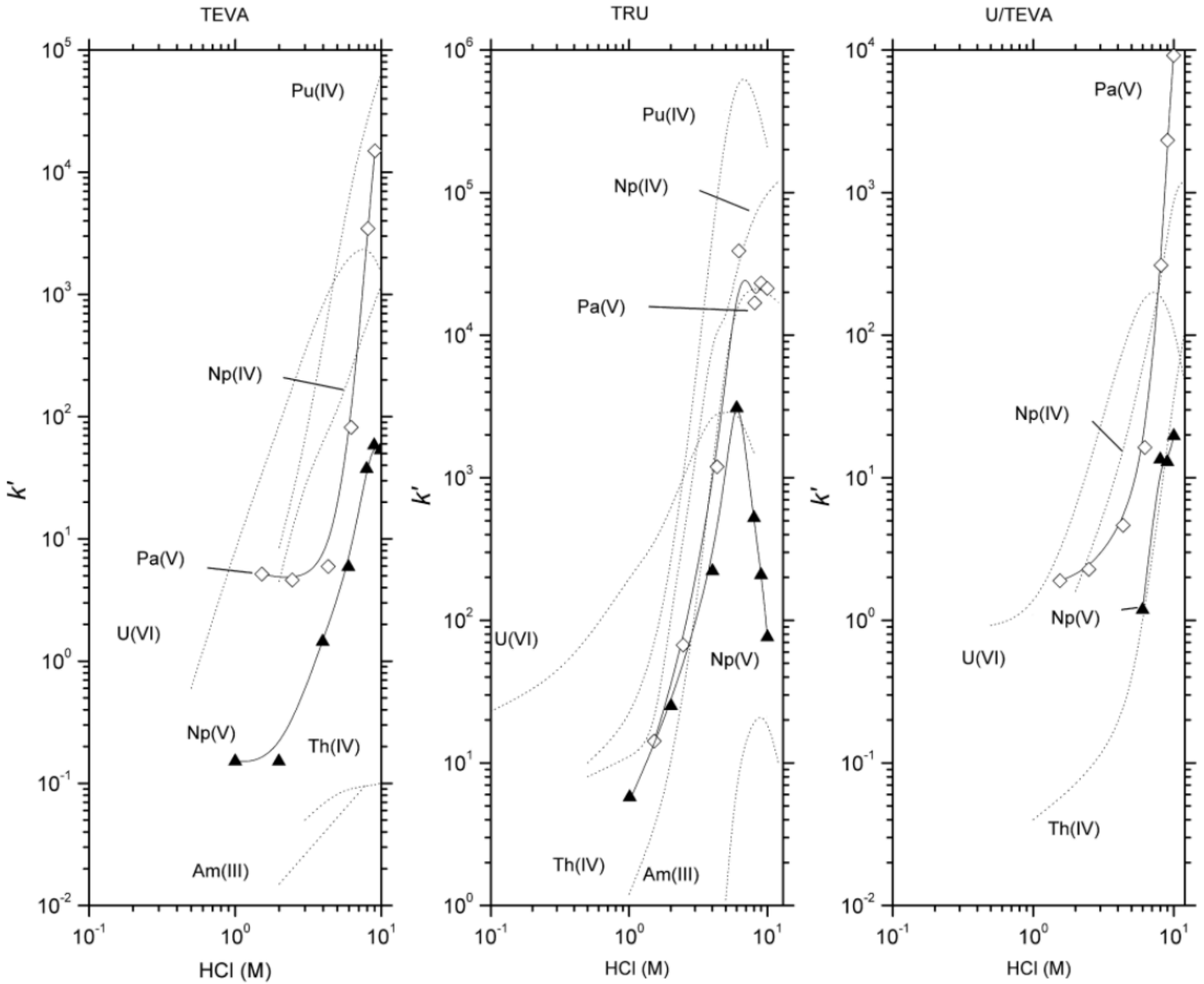

Fig. 2. HCl dependencies of k' values for selected actinides with the TEVA, TRU and U/TEVA resins (T= 22–26° C; 100–150 μm particle size resins). U(VI), Np(IV), Th(IV), Pu(IV) and Am(III) k' values are extracted from Refs. [18–20].